Innovative Structural Design and Coupled Vibration Analysis of the Bionic Hydraulic Pipeline

Changhong Guo*, Shaodong Wu*, Lingxiao Quan* and Ruxia Bai*

Yanshan University, College of Mechanical Engineering, Qinhuangdao, China*
E-Mail: lingxiao@ysu.edu.cn

Aiming at the vibration produced by the hydraulic pipeline system during operation, a bionic hydraulic pipeline with three layers of structure is developed based on the animal biological mechanism. The 14 - equation of hydraulic pipeline is perfected and the fluid-structure interaction dynamic model suitable for the bionic hydraulic pipeline is deduced. The two-way fluid-structure interaction analysis of the ANSYS simulation software shows the bionic hydraulic pipeline has better effect on absorbing pulsation and suppressing vibration. The results will provide a new technical approach for obtaining better vibration control effect.

Keywords: Absorption pulsation, Suppression vibration, bionic, Fluid-structure interaction, 14 - equation
Target audience: Hydraulic system, Fluid-structure interaction, Bionic

1 Introduction

High speed and high pressure will be one of the main development trends of hydraulic transmission system in the next twenty years/1/. It will aggravate the vibration of hydraulic pipeline system and reduce the working performance and reliability of the hydraulic control system. Axial piston pump is considered as one main source of the hydraulic system/2/, and more than 50% of the vibration is generated by it. Most of the flow pulsation and mechanical vibration generated by axial piston pump will transmit to the system through the hydraulic pipeline/3/. Therefore, absorbing flow pulsation to suppress vibration has become an important direction in the research of hydraulic pipeline vibration control in recent years.

Several common pulsation elimination devices in hydraulic pipeline system, such as the accumulator, H filter, high frequency on-off valve and pipeline attenuator, can be divided into passive control, semi-active control and active control according to the control mode. These devices and vibration control ideas lay a good foundation for the flow pulsation absorption of axial piston pump/4/. But these devices have the following deficiencies. Most of the devices are installed in the pipeline in parallel, which will excite the broadband secondary pulsation wave which is not conducive to absorption. Most devices have the characteristics of complex structure, many fault points and low reliability.

Comparing the hydraulic power system and the animal blood circulatory system, it can be found that there are many similarities between them. If the hydraulic pump is regarded as the heart of the system, then the hydraulic pipeline is the blood vessel of the system. The research results of absorption flow pulsation and vibration control of hydraulic pipeline at domestic and foreign are summarized in this paper. Referring to the biological mechanism that the left ventricular outflow vessels of the cheetah can tolerate blood pulsation with high pressure and high frequency, a bionic hydraulic pipeline is proposed, which provides a new idea for the vibration control of the hydraulic pipeline.

2 Structure and principle of the bionic hydraulic pipeline

Study on cardiovascular biology has found that when a quadruped, such as a cheetah, is chasing a prey, the heart beats violently and the blood pulsation amplitude and frequency increase instantaneously. The blood vessels are undamaged under blood flow pulsation with high frequency and high pressure, which benefits from the unique physiological structure. The cardiac outlet vessels of cheetah are composed of three layers: intima, media and adventitia. The structure is shown in figure 1. The intima is smooth and the resistance is smaller. The media with better structure adaptability can greatly improve the ability of blood vessel to absorb blood pulsation with high frequency and large amplitude. The adventitia contains large amounts of collagen fibrils that protect the vessel from breaking under high pressure/5/. The structure adaptability study of bionic blood vessels has shown that viscoelasticity of blood vessel has obvious effect on decreasing blood pulsation/6, 7, 8/.

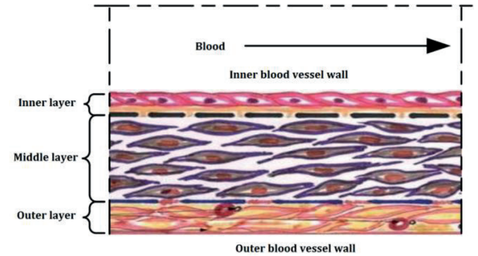

Figure 1 Schematic diagram of blood vessel wall

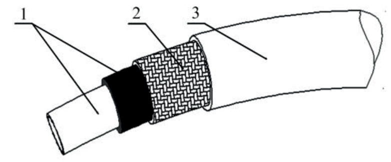

1. Inner layer 2. Middle level 3. Outer layer

Figure 2 Structure schematic diagram of the bionic hydraulic pipeline

The rubber, a kind of viscoelastic material, has physical and chemical properties which are different from metallic materials. Its mechanical properties are obviously nonlinear/9, 10/, and it is mainly used for vibration reduction and sealing in engineering applications. Therefore, according to the cardiovascular biological achievement that the cardiac outlet vessels can tolerate the blood pulsation with high frequency and large amplitude, a bionic hydraulic pipeline with three layers structure is proposed in this paper to absorb the flow pulsation at the hydraulic pump outlet and to suppress the pipeline vibration. The structure schematic diagram of the bionic hydraulic pipeline is shown in figure 2. The inner layer composed of nanometre coating materials and coating matrix is quite smooth and has a good ability to stabilize the flow of oil. The middle layer with good structure adaptability is woven from viscoelastic material, such as rubber, silica gel and so on. The outer layer is a high strength protective layer.

3 The fluid-structure interaction dynamic model

Fluid-structure interaction (FSI) is characterized by friction coupling, Poisson coupling, junction coupling and Bourdon coupling/11/, in which Poisson coupling and junction coupling have greater influence/12/. According to the solution of the control equation, it can be divided into the strong coupling of the direct solution and the weak coupling of the partitioned iterative solution/13/. A single straight pipeline is studied as the research object in this paper, so the friction coupling, junction coupling and Bourdon coupling can be neglected, and the Poisson coupling problem is mainly discussed. The strong coupling of direct solution is used during research.

The inner layer of bionic hydraulic pipeline is smooth. If the inner surface of the rubber material is set as smooth, the inner layer cannot be added to the model. The outer layer is a high strength protective layer of stainless steel. Therefore, the bionic hydraulic pipeline model is divided into two layers, as shown in figure 3. As a comparison, the ordinary stainless steel pipeline has only one layer, and the pipeline model is shown in figure 4.

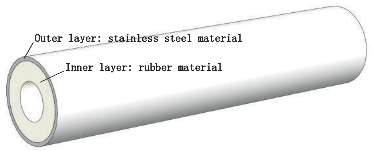

Figure 3 The model diagram of bionic hydraulic pipeline

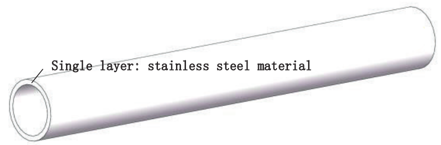

Figure 4 The model diagram of ordinary stainless steel pipeline

The coordinate system of the straight pipeline with a silica gel layer in figure 3 is established according to the right-hand rule. The force schematic diagram of bionic hydraulic pipeline is shown in figure 5.

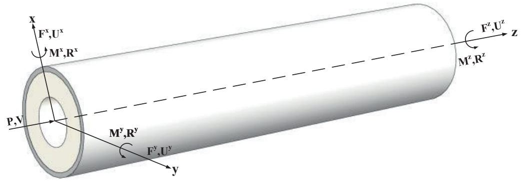

Figure 5 Force schematic diagram of bionic hydraulic pipeline

In order to establish the dynamic model, we assume that the pipeline is installed parallel to the horizontal plane and consider the influence of the gravity inertia and the fluid viscous friction. Referring to the 14 - equation model of fluid-structure interaction/14/, the dynamic model of bionic hydraulic pipeline is as follows:

3.1 The motion of the axial pipeline and the fluid

3.1.1 The fluid motion differential equation

A motion element of fluid dz is shown in Fig. 6 and its fluid motion differential equation is expressed as

$$\left(P+\frac{\partial P}{\partial z}dz-P\right)A_f+f=-\rho_f A_f dz\frac{\partial V}{\partial t}, \tag{1}$$

in which $f=2\pi r_r \tau \mathrm{dz}$.

After simplification, the fluid motion equilibrium equations along the axial direction are as follows.

$$\frac{\partial V}{\partial t}+\frac{1}{\rho_f}\frac{\partial P}{\partial z}=-\frac{2\pi r_r \tau}{\rho_f A_f}. \tag{2}$$

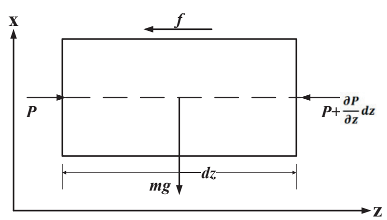

Figure 6 A motion element of fluid

3.1.2 The relationship between pipeline deformation and fluid pressure

If the fluid pressure is P, the pressure on the inner wall of the rubber layer is also P. Supposed that the pressure on the stainless steel layer is P_P. The relationship between P_P and P is

$$2\pi r_r P-k_r\frac{\partial \lambda}{\partial t}-\zeta_r\frac{\partial^2 \lambda}{\partial t^2}-2\pi r_P P_P=0. \tag{3}$$

So,

$$P_P=\frac{r_r}{r_P}P-\frac{k_r}{2\pi r_P}\frac{\partial \lambda}{\partial t}-\frac{\zeta_r}{2\pi r_P}\frac{\partial^2 \lambda}{\partial t^2}. \tag{4}$$

The equation (4) shows that the pressure on the outer wall of the bionic hydraulic pipeline is less than the fluid pressure, while the pressure on the outer wall of the stainless steel pipeline is equal to the fluid pressure. So, compared with the ordinary stainless steel pipeline, the Poisson coupling effect of bionic hydraulic pipeline is smaller.

The stainless steel layer is considered as thin shell. For the thin-walled pipeline, the stress state of pipeline wall is two directional. On the one hand, the pressure can cause circumferential normal stress σ_θ; on the other hand, it can also cause the axial normal stress σ_z. The σ_θ and σ_z can be described as

$$\sigma_\theta=\frac{P_P r_P}{e}, \tag{5}$$

$$\sigma_z=\frac{F^z}{A_P}. \tag{6}$$

And

$$\frac{\partial \sigma_z}{\partial t}=\frac{E}{1-\mu^2}\left(\frac{\partial \varepsilon_z}{\partial t}+\mu\frac{\partial \varepsilon_\theta}{\partial t}\right), \tag{7}$$

$$\frac{\partial \sigma_\theta}{\partial t}=\frac{E}{1-\mu^2}\left(\frac{\partial \varepsilon_\theta}{\partial t}+\mu\frac{\partial \varepsilon_z}{\partial t}\right). \tag{8}$$

In the formula (8),

$$\frac{\partial \varepsilon_z}{\partial t}=\frac{\partial U^z}{\partial z}, \tag{9}$$

$$\frac{\partial \varepsilon_\theta}{\partial t}=\frac{1}{r_P}\frac{\partial H}{\partial t}. \tag{10}$$

Assuming $k_r=0$ and $\zeta_r=0$, by analysing equations (5) - (8), the relationship can be expressed as

$$\frac{\partial U^z}{\partial z}-\frac{1}{EA_P}\frac{\partial F^z}{\partial t}+\frac{\mu r_r}{Ee}\frac{\partial P}{\partial t}=0. \tag{11}$$

3.1.3 The axial motion equation of pipeline

A motion element of fluid dz is shown in figure 7, and the axial motion equation of pipeline is

$$\left(F^z+\frac{\partial F^z}{\partial z}dz-F^z\right)+f=\frac{\partial U^z}{\partial t}(\rho_P A_P+\rho_r A_r)dz, \tag{12}$$

in which $f=2\pi r_r \tau \mathrm{dz}$.

The axial motion equation of the pipeline is simplified as follows.

$$\frac{\partial U^z}{\partial t}-\frac{1}{\rho_P A_P+\rho_r A_r}\frac{\partial F^z}{\partial z}=\frac{2\pi r_r \tau}{\rho_P A_P+\rho_r A_r} \tag{13}$$

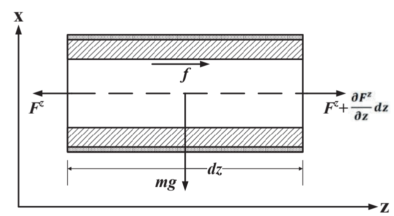

Figure 7 A motion element of pipeline

3.1.4 The continuity equation of fluid

The fluid volume in the pipeline element increases ΔV per unit time, and the ΔV is

$$\Delta V = -A_f \frac{\partial V}{\partial z} dz. \tag{14}$$

The increased fluid is filled into the three parts of the space.

ΔV_1 means the change of volume due to fluid compressibility, which is expressed as

$$\Delta V_1 = \frac{1}{K_f} A_f dz \frac{\partial P}{\partial t}. \tag{15}$$

ΔV_2 is the change of volume caused by compression of rubber layer, which is

$$\Delta V_2 = 2\pi r_r^2 \frac{\partial \lambda}{\partial t} dz. \tag{16}$$

ΔV_3 is the change of volume caused by deformation of stainless steel layer, which is described as

$$\Delta V_3 = 2\pi r_P \frac{\partial Y}{\partial t} dz. \tag{17}$$

The volume change can be expressed as $\Delta V = \Delta V_1 + \Delta V_2 + \Delta V_3$, so the equation is

$$\frac{\partial V}{\partial z} + \left(\frac{1}{K_f} + \frac{2R(1-\mu^2)}{eE}\right)\frac{\partial P}{\partial t} - \frac{2\mu}{EA_P}\frac{\partial F^z}{\partial t} + 2\frac{\partial \lambda}{\partial t} = 0. \tag{18}$$

3.2 Shear and bending in the y-z plane:

The rotation angle of pipeline is caused by two aspects: one is the bend R^z of the pipeline itself; the other is pipeline deformation β^z due to shearing force.

The rotation angle of pipeline caused by shearing force is:

$$\beta^z = \frac{F^y}{A_P G_P + A_r G_r}. \tag{19}$$

So,

$$\frac{dy}{dz} = -R^z - \beta^z. \tag{20}$$

The next equation can be obtained by differentiating the two sides of formula (20) with respect to time.

$$\frac{\partial F^y}{\partial t} - (A_P G_P + A_r G_r)\left(\frac{\partial U^y}{\partial z} + R^x\right) = 0 \tag{21}$$

The relationship between the rotation angle and the bending moment of the pipeline around the X-axis is as follows:

$$\frac{M^x}{E_P I_P + E_r I_r} = \frac{\partial R^x}{\partial z} \tag{22}$$

The two sides of formula (22) is differentiated with respect to time, obtaining the result

$$\frac{\partial M^x}{\partial t} - (E_P I_P + E_r I_r)\frac{\partial R^x}{\partial z} = 0 \tag{23}$$

According to the Newton's second law, the force balance in the Y direction is deduced.

$$\frac{\partial F^y}{\partial z} - \left(\rho_P A_P + \rho_f A_f + \rho_r A_r\right)\frac{\partial U^y}{\partial t} = 0 \tag{24}$$

The moment balance equations of pipeline in the X direction can be expressed as

$$\frac{\partial M^x}{\partial z} - F^y - (\rho_P I_P + \rho_f I_f + \rho_r I_r)\frac{\partial R^x}{\partial t} = 0. \tag{25}$$

When deducing the relationship between shearing force and bending moment in the y-z plane, some parameters of rubber, such as shear modulus and inertia moment, are included in the formula because there is a rubber layer in the bionic pipeline.

3.3 Shear and bending in the x-z plane

The derivation process of formula is the same as 3.2 and the results are shown as

$$\frac{\partial M^y}{\partial z} + F^x - (\rho_P I_P + \rho_f I_f + \rho_r I_r)\frac{\partial R^y}{\partial t} = 0 \tag{26}$$

$$\frac{\partial M^y}{\partial t} - (E_P I_P + E_r I_r)\frac{\partial R^y}{\partial z} = 0 \tag{27}$$

$$\frac{\partial F^x}{\partial z} - \left(\rho_P A_P + \rho_f A_f + \rho_r A_r\right)\frac{\partial U^x}{\partial t} = 0 \tag{28}$$

$$\frac{\partial F^x}{\partial t} - (A_P G_P + A_r G_r)\left(\frac{\partial U^x}{\partial z} - R^y\right) = 0 \tag{29}$$

3.4 The torque at the pipeline wall

The constitutive relationship between the rotation angle and torque can be obtained.

$$\frac{\partial R^z}{\partial z} - \frac{1}{G_P J_P + G_r J_r}\frac{\partial M^z}{\partial t} = 0 \tag{30}$$

According to the axial torque balance equation, there is

$$\frac{\partial M^z}{\partial z} - (\rho_P J_P + \rho_r J_r)\frac{\partial R^z}{\partial t} = 0. \tag{31}$$

Similarly, the shear modulus and polar inertia moment of the rubber are included in the formula because of the rubber layer in the pipeline.

3.5 The compression of the rubber layer

The rubber layer of the bionic hydraulic pipeline is hollow cylinder/10/. The relationship between the cross sectional compression λ and the fluid pressure P under pressure is

$$\lambda = \frac{P(r_P^2 - r_r^2)}{K_r r_r}. \tag{32}$$

The Mooney-Rivlin model with two parameters is used as the constitutive model of the rubber layer in the bionic pipeline. If $C_{10} = 0.2\text{MPa}$ and $C_{01} = 1.4\text{MPa}$, the bulk modulus of rubber material is approximately

$$K_r = 5.487 \times 10^6 \lambda + 1.334 \times 10^8. \tag{33}$$

The bulk modulus of rubber is much smaller than that of stainless steel, so it is easier to deform under compression. The outlet pressure curve of axial piston pump is approximately a sine curve. When the pressure of the fluid increases, the compression of the rubber layer in the bionic hydraulic pipeline becomes larger; the fluid region in the pipeline becomes larger and the velocity of the fluid becomes smaller relatively. When the pressure decreases, the rubber expands; the fluid region in the pipeline becomes smaller and the velocity of the fluid becomes larger than before. If the fluid flows through the bionic hydraulic pipeline, its flow fluctuation will be smaller. In addition, the Poisson coupling effect of the outer layer in the bionic hydraulic pipeline is weakened. Therefore, the bionic hydraulic pipeline can achieve the purpose of absorbing the flow pulsation and suppressing the system vibration.

4 The frequency domain characteristics solution for fluid-structure interaction dynamic model of bionic hydraulic pipeline

The frequency components of the pipeline can be found out by solving the frequency domain characteristics of the hydraulic pipeline so as to provide reference for avoiding the resonance failure of the pipeline. The frequency domain solution of Laplace transform proposed by Zhang Lixiang has good generality. So the Laplace transform will be used in this paper to convert the partial differential equation of the fluid-structure interaction dynamic model into the frequency domain equation that can be solved further.

If $\Phi(z,t)$ means a vector composed of kinetic parameters of medium and pipeline along the axis, it can be expressed as

$$\Phi(z,t) = (V, P, U^z, F^z, U^y, F^y, R^x, M^x, U^x, F^x, R^y, M^y, R^z, M^z, \lambda)^T \tag{34}$$

The relationship of state variables between the pipeline at any position z and at the position 0 can be represented by the domain transfer matrix $\boldsymbol{M}(z,s)$.

$$\overline{\boldsymbol{\Phi}}(z,s) = \boldsymbol{M}(z,s)\overline{\boldsymbol{\Phi}}(0,s) \tag{35}$$

For the pipeline with length L, its state variables at any position can be solved by using the domain transfer matrix and boundary conditions. There are seven boundary conditions respectively for the two ends of a single pipeline (z=0 and z=L), and the general expressions are as follows.

$$[\boldsymbol{D}_0(s)]_{7\times14}[\overline{\boldsymbol{\Phi}}(0,s)]_{14\times1} = [\boldsymbol{Q}_0(s)]_{7\times1} \tag{36}$$

$$[\boldsymbol{D}_L(s)]_{7\times14}[\overline{\boldsymbol{\Phi}}(L,s)]_{14\times1} = [\boldsymbol{Q}_L(s)]_{7\times1} \tag{37}$$

Among them, $D_0(s)$ and $D_L(s)$ are the boundary matrix at both ends of the pipeline; $Q_0(s)$ and $Q_L(s)$ are the excitation matrix at both ends of the pipeline; the subscripts outside square brackets are for rows and columns of matrix respectively.

According to the formula (35) - (37), the state variable of the pipeline at the end of z=0 is

$$\overline{\boldsymbol{\Phi}}(0,s) = \begin{bmatrix} \boldsymbol{D}_0(s) \\ \boldsymbol{D}_L(s)\boldsymbol{M}(L,s) \end{bmatrix}^{-1} \begin{bmatrix} \boldsymbol{Q}_0(s) \\ \boldsymbol{Q}_L(s) \end{bmatrix} \tag{38}$$

5 Solution of dynamic model

If the ends of pipeline are free and full of oil; both ends are blocked; the friction between the inner wall of silica gel layer and the fluid is ignored, the physical parameters of pipeline and fluid are shown in table 1.

	Stainless steel	Silica gel	Fluid	Plug
length (m)	0.5	0.5		
inner radius (m)	0.02	0.005		
wall thickness (m)	0.002	0.015		
Poisson ratio	0.3	0.49		
density (kg/m^3)	7930	1100	872	
Young modulus (Pa)	1.94×10^{11}			
C_{10} (MPa)		0.2		
C_{01} (MPa)		1.4		
quality (kg)				0.25

Table 1 Structural and material parameters of pipeline model

A mechanical shock excitation is applied to the initial end of the pipeline. The average size is F=15000N; the time is T=0.002s, and the expression is

$$F = [1(t) - 1(t-T)] \tag{39}$$

The corresponding excitation vector is:

$$\begin{cases} \boldsymbol{Q}_0(s) = \begin{bmatrix} 0 & -\left(\frac{F}{s}\right)(1-\mathrm{e}^{-sT}) & 0 & 0 & 0 & 0 & 0 \end{bmatrix}^{\mathrm{T}} \\ \boldsymbol{Q}_L(s) = \begin{bmatrix} 0 & 0 & 0 & 0 & 0 & 0 & 0 \end{bmatrix}^{\mathrm{T}} \end{cases} \tag{40}$$

The fluid-structure interaction dynamic model of bionic hydraulic pipeline is programmed and solved in MATLAB. The radial pressure frequency characteristic curve and the axial velocity frequency characteristic curve at the initial end of pipeline are shown in figure 8 and figure 9.

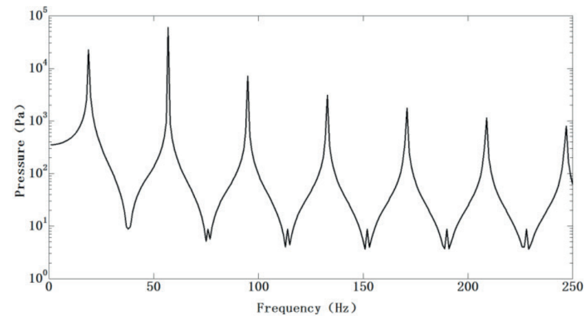

Figure 8 The radial pressure frequency characteristic curve

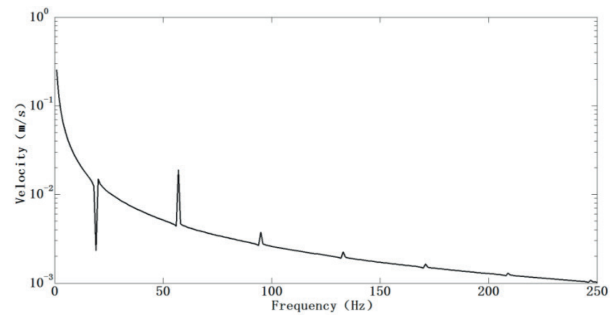

Figure 9 The axial velocity frequency characteristic curve

6 Simulation analysis

The pipeline models of figure 3 and figure 4 are imported into the ANSYS WORKBENCH software respectively to analyse the two-way fluid-structure interaction. The parameters of pipeline model are shown in table 1. The two ends of the pipeline are clamped and the friction between wall and fluid is neglected. The fluid is 10# aviation hydraulic oil; the density is 870 kg/m^3; the kinetic viscosity is 0.0087 kg/ (m·s). The fluid is modelled by a standard k-ε turbulence model

When the outlet pressure of axial piston pump is 9MPa, the flow pulsation curve is shown in figure 10.

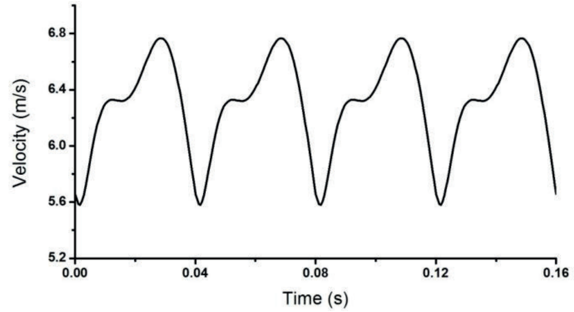

Figure 10 The flow pulsation curve of axial piston pump outlet

The flow pulsation shown in figure 10 is used as the inlet flow condition of the pipeline, and the outlet pressure of the pipeline is set to 9MPa.

The fluid-structure interaction vibration characteristics of the above model are analyzed. The flow pulsation curve at the outlet of bionic hydraulic pipeline and common stainless steel pipeline is shown in figure 11. The vibration amplitude curves of the wall middle joint of the bionic hydraulic pipeline and common stainless steel pipeline are shown in figure 12.

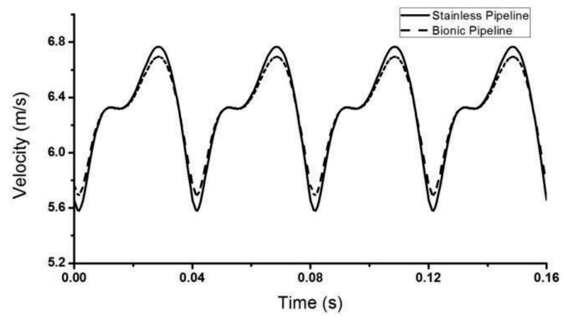

Figure 11 The velocity pulsation curve of different pipelines outlet

It can be seen from figure 11 that the outlet flow of the two pipelines is still periodic pulsation. The flow pulsation amplitude of bionic hydraulic pipeline outlet decreases after absorbed by pipeline, while the flow pulsation amplitude of stainless steel hydraulic pipeline outlet is basically the same as the inlet flow amplitude. It is shown that the pulsating amplitude will decrease when the pulsating fluid flows through the bionic hydraulic pipeline. The bionic hydraulic pipeline has good effect on the absorption of flow pulsation.

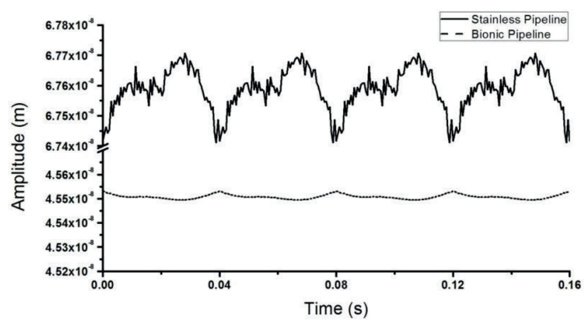

Figure 12 The vibration amplitude curves of the wall middle joint of different hydraulic pipelines

It can be seen from figure 12 that the vibration amplitude of the wall middle joint of the bionic hydraulic pipeline is smaller than that of the stainless steel hydraulic pipeline. It shows that the bionic hydraulic pipeline can suppress the pipeline vibration while absorbing the flow pulsation.

7 Summary and Conclusion

Based on the mechanism of animal biology, a bionic hydraulic pipeline with three layers is created. It is directly connected with the hydraulic pump, so it will not excite the secondary high frequency pulsation, which makes up for the shortcomings of the traditional vibration control means. The research results provide a new technical way to break through the mechanism that absorption pulsation to suppress vibration and to obtain better vibration control effect.

On the basis of the original 14 - equation, the 14 - equation suitable for the bionic hydraulic pipeline is derived in this paper. The equation is successfully solved and the correctness of the new equation is verified. In addition, the simulation analysis shows that the bionic hydraulic pipeline has better capacity of absorbing flow pulsating and suppressing pipeline vibration than the ordinary stainless steel pipeline.

Nomenclature

Variable	*Description*	*Unit*
A	Cross-sectional area	[m^2]
E	Modulus of elasticity	[Pa]
e	Thickness of outer layer	[m]
F	Force	[N]
G	Shear modulus of rigidity	[Pa]
I	Moment of inertia	[m^4]
J	Polar moment of inertia	[m^4]
K	Bulk modulus of elasticity	[Pa]
M	Moment	[N·m]
P	Pressure	[Pa]
R	Rotational velocity	[rad/s]
r	Radius of cross-section	[m]
U	Velocity of pipeline	[m/s]
V	Velocity of liquid	[m/s]
ρ	Mass density	[kg/m^3]
μ	Poisson ratio	[-]
z	Principal directions	[-]
t	Time	[s]
τ	Friction between fluid and inner layer	[-]
Y	Radial variable of outer layer	[m]

λ	Deformation of inner layer	[m]
k	Linear stiffness	[N/m]
ζ	Linear damping	[N·s/m]
C_{10}, C_{01}	Material constant	[MPa]
Superscripts		
x, y, z	Principal directions	[-]
Subscripts		
f	Fluid	[-]
P	Outer layer	[-]
r	Inner layer	[-]

References

/1/ China Hydraulics Pneumatics & Seals Association, 流体动力传动与控制技术路线图, Science and Technology of China Press, Beijing, China, 2012.

/2/ Lingxiao Quan, Hongliang Luo, Jin Zhang, 斜轴式轴向柱塞泵壳体结构振动谐响应分析, In: Chinese Hydraulics & Pneumatics, pp. 33-39, 2014.

/3/ Zhanlin Wang,飞机高压液压能源系统, Beijing University of Aeronautics and Astronautics Press, Beijing, China, 2004.

/4/ Lingxiao Quan, Xiangdong Kong, Yingjie Gao, 不考虑进口特性的蓄能器吸收冲击理论及试验, In: Journal of Mechanical Engineering, Vol. 43, No. 7, pp. 28-32, 2007.

/5/ George Zorbas, Theodoros Samaras, *A study of the sink effect by blood vessels in radiofrequency ablation*, In: Computers in Biology and Medicine, pp. 182-186, 2015.

/6/ Venkatraman S, Boey F, Lao LL, *Implanted cardiovascular polymers: Natural, synthetic and bio-inspired*, In: Progress in Polymer Science, Vol. 33, No. 9, pp. 853-874, 2008.

/7/ Yu Y, Perdikaris P, Karniadakis G E, *Fractional modeling of viscoelasticity in 3D cerebral arteries and aneurysms*, In: Journal of Computational Physics, pp. 219-242, 2016.

/8/ Lukáčová-Medvid'Ová M, Rusnáková G, Hundertmark-Zaušková A, *Kinematic splitting algorithm for fluid–structure interaction in hemodynamics*, In: Computer Methods in Applied Mechanics & Engineering, Vol. 265, No. 3, pp. 83-106, 2013.

/9/ Liao K, Hu C, Sueyoshi M., *Free surface flow impacting on an elastic structure: Experiment versus numerical simulation*, In: Applied Ocean Research, pp. 192-208, 2015.

/10/ Sahu R K, Patra K, *Estimation of Elastic Modulus of Dielectric Elastomer Materials Using Mooney-Rivlin and Ogden Models*, In: Advanced Materials Research, Vol. 685, No. 1, pp. 331-335, 2013.

/11/ Richter T., Wick T., *Finite elements for fluid-structure interaction in ALE and fully Eulerian coordinates*, In: Computer Methods in Applied Mechanics and Engineering, Vol. 199, No. 41, pp. 2633-2642, 2010.

/12/ Li S, Karney B W, Liu G, *FSI research in pipeline systems – A review of the literature*, In: Journal of Fluids & Structures, pp. 277-279, 2015.

/13/ Ruojun Qian, Shilin Dong, Xingfei Yuan, 流固耦合理论研究进展, In: Spatial Structures, Vol. 14, No. 1, pp. 6-18, 2008.

/14/ Wiggert D C, Hatfield F J, Stuckenbruck S, *Analysis of Liquid and Structural Transients in Piping by the Method of Characteristics*, In: Journal of Fluids Engineering, Vol. 109, No. 2, pp. 161-165, 1987.

/15/ Lixiang Zhang, Ke Yang, 流体结构互动理论及其应用, Science Press, Beijing, China, 2004.